JAMES | Journal of Advances in Modeling Earth Systems

RESEARCH ARTICLE
10.1029/2023MS003866

Implementation and Exploration of Parameterizations of Large-Scale Dynamics in NCAR's Single Column Atmosphere Model SCAM6

S. Cohen[1], A. Sobel[1], M. Biasutti[1], S. Wang[2], I. Simpson[3], A. Gettelman[3,4], and I. Hu[5,6]

[1]Columbia University, New York, NY, USA, [2]Nanjing University, Nanjing, China, [3]NSF National Center for Atmospheric Research, Boulder, CO, USA, [4]Pacific Northwest National Laboratory, Richland, WA, USA, [5]CIRES, University of Colorado, Boulder, CO, USA, [6]Physical Sciences Laboratory, NOAA, Boulder, CO, USA

Key Points:

- We use three different methods to parameterize the large-scale (LS) dynamics in NCAR's single column atmospheric model (SCAM6)
- As in the Global Atmospheric System Studies Intercomparison, we test SCAM6's response to various boundary conditions and model parameters
- Under all three methods, circulation strength is decreased when barriers to convection are reduced

Correspondence to:

S. Cohen,
sean.cohen@columbia.edu

Citation:

Cohen, S., Sobel, A., Biasutti, M., Wang, S., Simpson, I., Gettelman, A., & Hu, I. (2024). Implementation and exploration of parameterizations of large-scale dynamics in NCAR's single column atmosphere model SCAM6. *Journal of Advances in Modeling Earth Systems*, *16*, e2023MS003866. https://doi.org/10.1029/2023MS003866

Received 8 JUN 2023
Accepted 24 MAR 2024

Abstract A single column model with parameterized large-scale (LS) dynamics is used to better understand the response of steady-state tropical precipitation to relative sea surface temperature under various representations of radiation, convection, and circulation. The large-scale dynamics are parametrized via the weak temperature gradient (WTG), damped gravity wave (DGW), and spectral weak temperature gradient (Spectral WTG) method in NCAR's Single Column Atmosphere Model (SCAM6). Radiative cooling is either specified or interactive, and the convective parameterization is run using two different values of a parameter that controls the degree of convective inhibition. Results are interpreted in the context of the Global Atmospheric System Studies -Weak Temperature Gradient (GASS-WTG) Intercomparison project. Using the same parameter settings and simulation configuration as in the GASS-WTG Intercomparison project, SCAM6 under the WTG and DGW methods produces erratic results, suggestive of numerical instability. However, when key parameters are changed to weaken the large-scale circulation's damping of tropospheric temperature variations, SCAM6 performs comparably to single column models in the GASS-WTG Intercomparison project. The Spectral WTG method is less sensitive to changes in convection and radiation than are the other two methods, performing qualitatively similarly across all configurations considered. Under all three methods, circulation strength, represented in 1D by grid-scale vertical velocity, is decreased when barriers to convection are reduced. This effect is most extreme under specified radiative cooling, and is shown to come from increased static stability in the column's reference radiative-convective equilibrium profile. This argument can be extended to interactive radiation cases as well, though perhaps less conclusively.

Plain Language Summary Single column models, as the name suggests, only model the vertical dimension of the atmosphere. They are simpler than full-scale 3D global circulation models, but nonetheless play an important role in model development and in better understanding physical phenomena. We use NCAR's Single Column Atmosphere Model (SCAM6) to better understand tropical rainfall. In a single column model, the atmospheric wind coming from other locations (the large-scale circulation) must be either specified or approximated using a parameterization. We implement three different parameterizations of the large-scale circulation into SCAM6 and assess how SCAM6 responds to various changes while using these parameterizations. The Global Atmospheric System Studies-Weak Temperature Gradient (GASS-WTG) Intercomparison project assessed the performance of various other single column models using two parameterizations of the large-scale circulation. We fold SCAM6 into this Intercomparison, and we find that SCAM6 performs substantially differently to its peers under the settings used in the GASS-WTG Intercomparison project, but more comparably to its peers when key circulation parameters are relaxed. Another notable finding is that, across all three parameterizations of large-scale dynamics, circulation strength decreases when we reduce SCAM6's barrier to convection.

1. Introduction

Single column models (SCMs) are one-dimensional (1D) models that only explicitly represent the vertical dimension of the atmosphere. While the column's full convective, radiative, and moist physics schemes are retained, the large-scale (LS) dynamics must be either specified or parameterized. While SCMs only represent a subset of the processes captured in full-scale 3D global circulation models (GCMs), they are part of model

hierarchies which can play important roles both in model development and in better understanding physical phenomena (Held, 2005).

Parameterizations of the LS dynamics have been developed primarily in the context of the tropical atmosphere. Due to the smallness of the Coriolis parameter near the equator, tropical horizontal free-tropospheric pressure and density gradients are weak (Charney, 1963). For some purposes, it can be assumed that LS dynamics will simply act to relax the column's temperature to a predefined profile representative of regions adjacent to the column, and by extension the tropics as a whole. This target profile is often modeled as a radiative convective equilibrium (RCE) solution over an appropriate sea surface temperature (SST), representing either the tropical mean or the mean over regions of frequent deep convection (Held et al., 1993; Jakob et al., 2019; Sobel & Bretherton, 2000; Sobel et al., 2002; Tompkins & Craig, 1998). In RCE, the LS vertical velocity is zero, meaning that radiative cooling balances convective heating at all pressure levels and column precipitation must equal column evaporation. Any given region within the real tropics can sustain precipitation greater or less than the tropical mean by importing or exporting moisture via the LS circulation. Parametrizations of LS dynamics try to capture this process, including its dependence on both external parameters (e.g., local SST) and internal ones (e.g., those that represent aspects of convective or radiative physics).

The goal of this paper is to test several parameterizations of LS dynamics in NCAR's Single Column Atmosphere Model, (SCAM6) (Gettelman et al., 2019), the SCM version of NCAR's Community Earth System Model, CESM2.2.0 (Danabasoglu et al., 2020). SCAM6 retains the full radiation, convection, and other physics schemes included in CESM2.2.0, but requires the LS circulation to be either specified or parameterized. We parameterize the circulation via the following methods: the weak temperature gradient (WTG) method (Raymond & Zeng, 2005; Sobel & Bretherton, 2000), damped gravity wave (DGW) method (Kuang, 2008), and the spectral weak temperature gradient (Spectral WTG) method (Herman & Raymond, 2014; S. Wang et al., 2016).

These parameterizations of LS dynamics have been implemented into various SCMs and cloud resolving models (CRMs). To date, the most comprehensive analysis of how the WTG and DGW methods perform across SCMs and CRMs is the Global Atmospheric Systems Study-Weak Temperature Gradient (GASS-WTG) Intercomparison project (Daleu et al., 2015, 2016), which assessed the steady-state response of 12 models to changes in relative SST (i.e., varying SST while holding the target tropospheric temperature profile fixed) using both WTG and DGW (but not Spectral WTG) methods. One goal of this study is to fold NCAR's Single Column Atmospheric Model into the results of the GASS-WTG Intercomparison project by implementing the same parameterizations of LS dynamics into SCAM6 and replicating the conditions applied by Daleu et al. (2016). The GASS-WTG Intercomparison project was important for interpreting discrepancies across models and for understanding the coupling between convection and LS tropical dynamics. For example, Daleu et al. (2016) find that discrepancies between published results can be related to the choice of the parametrization of LS dynamics and that simulations with explicit convection have more constrained behavior than those with parametrized convection. By including SCAM6 in this intercomparison, we seek to better understand how SCAM6 compares to other SCMs and CRMs and to leverage SCAM6's reduced dimensionality to better understand how convection and LS dynamics interact in the tropics. We will also assess how the Spectral WTG method compares to the WTG and DGW methods in SCAM6, and analyze how the circulation responds to changes to the radiative and convective schemes. Since SCAM6 is primarily a tool for model development (Gettelman et al., 2019), the analysis of these idealized simulations may also serve to inform future development of Community Earth System Model (CESM).

Under the conditions applied in the GASS-WTG Intercomparison project, the WTG and DGW methods produce erratic results in SCAM6, suggestive of numerical instability (see Results). Thus, we alter key parameters in these methods to improve performance and subsequently present four different configurations of the convection and radiation schemes in SCAM6: (a) specified radiation with inhibited convection (RsCi), (b) specified radiation with uninhibited convection (RsCu), (c) interactive radiation with inhibited convection (RiCi), and (d) interactive radiation with uninhibited convection (RiCu). Specifically in this study, specified radiation refers to the idealized radiative cooling profile used in Daleu et al. (2016) and interactive radiation refers to the radiation modeled by the default radiation package in SCAM6. Likewise, “inhibited” and “uninhibited” convection refer to different values of a parameter in SCAM6's deep convection scheme that controls the number of model levels over which a rising parcel can experience negative buoyancy before deep convection is suppressed. This parameter is shown to have important effects in RCE simulations by Hu et al. (2022). We include specified radiation cases for better comparison between SCAM6 and the SCMs in Daleu et al. (2016), and we include interactive radiation cases for better

assessment of the overall performance of SCAM6 under parameterized LS dynamics (PLSD) and of the interaction between its radiation and convection schemes.

This paper is organized as follows. The Methods section describes the details of each parameterization implemented into SCAM6 (WTG, DGW, and Spectral WTG methods). It also outlines the model set up and each of the four different configurations of the convection and radiation schemes (RsCi, RsCu, RiCi, and RiCu). The Results section discusses the performance of each parameterization under the conditions given in Daleu et al. (2016). To avoid numerical instability, we also relax key circulation parameters and assess the sensitivity of the WTG, DGW, and Spectral WTG methods to changes in the radiation and convection schemes. The Discussion section presents key takeaways regarding the relative performance of each parameterization of LS dynamics under the configurations considered and regarding important mechanistic feedbacks between the circulation, convection and radiation schemes. Finally, the Conclusion section summarizes the study and assesses its relevance to NCAR's GCM CESM2.2.0 and to tropical precipitation more broadly.

2. Methods

2.1. Parameterizations of Large-Scale Dynamics

This study considers three parameterizations of LS dynamics: the WTG method (Raymond & Zeng, 2005; Sobel & Bretherton, 2000), the DGW method (Kuang, 2008, 2011), and the spectral WTG (Spectral WTG) method (Herman & Raymond, 2014; S. Wang et al., 2016).

In the WTG method, we neglect the horizontal advection and time dependent terms from the column's temperature equation, and represent adiabatic warming or cooling due to vertical motion by a Newtonian relaxation of the domain-mean virtual potential temperature in the column, $\overline{\theta_v}$, back to the target profile, $\overline{\theta_v^{\mathrm{ref}}}$, on a time scale, τ. The LS pressure velocity, $\overline{\omega}$, is then diagnosed according to Raymond and Zeng (2005):

$$\overline{\omega}\frac{\partial \overline{\theta_v}}{\partial p} = \frac{\left(\overline{\theta_v} - \overline{\theta_v^{\mathrm{ref}}}\right)}{\tau}$$

The WTG approximation breaks down in the boundary layer due to the effects of surface turbulent fluxes of heat and momentum. The LS pressure velocity ought to nearly vanish at the surface in steady state, so we linearly interpolate $\overline{\omega}$ from its value at 850 Pa to zero at the surface, as is done in Daleu et al. (2016). In addition, to avoid numerical issues, we place a lower limit of 2×10^{-4} K Pa^{-1} on the absolute value of the static stability, $\frac{\partial \overline{\theta_v}}{\partial p}$ (Raymond & Zeng, 2005), used in the calculation of $\overline{\omega}$.

The DGW method attempts to more explicitly capture the gravity wave dynamics that act to relax the zonal momentum of the column back to the tropical mean. Using the 2D anelastic nonrotational momentum, continuity, and hydrostatic equations, the DGW method applies a wave equation for $\overline{\omega}$. At each time step, a single linear gravity wave of specified horizontal wave number, k, minimizes deviations in virtual temperature, $\overline{T_v}$, from the target profile, $\overline{T_v^{\mathrm{ref}}}$ (Kuang, 2008, 2011):

$$\frac{\partial}{\partial p}\left(\epsilon \frac{\partial \overline{\omega}}{\partial p}\right) = \frac{k^2 R_D}{p^{\mathrm{ref}}}\left(\overline{T_v} - \overline{T_v^{\mathrm{ref}}}\right)$$

here, R_D is the gas constant of dry air and ϵ is the specified mechanical damping coefficient. We exclude the time derivative on the left-hand side since we are primarily concerned with the column's steady state response. We apply homogeneous boundary conditions for $\overline{\omega}$ at the surface and at a nominal upper boundary (100 hPa), and solve the resulting ordinary differential equation at each time step using a standard triangular matrix solver. As in Daleu et al. (2016), we set the horizontal wave number, k, to 10^{-6} m^{-1}, corresponding to a wavelength of about 6,000 km.

The spectral WTG method also uses gravity wave dynamics to capture more accurately the LS relaxation to the target temperature profile. Recognizing that gravity waves of different wavelengths will travel at different speeds, the spectral WTG method damps each spectral mode's temperature forcing proportionally to that mode's

theoretical gravity wave speed (Herman & Raymond, 2014). Following S. Wang et al. (2016), who used a slightly different approximation than Herman and Raymond (2014), we derive these spectral modes and their corresponding theoretical wave speeds by constructing an equation for the vertical velocity, again assuming a 2D non-rotating anelastic atmosphere. Homogeneous boundary conditions enforce that the vertical velocity vanish at the surface and at the tropopause, and Boussinesq-like assumptions eliminate any single derivatives in the vertical velocity, $\overline{w}$:

$$(\rho\overline{w})_{zz} + \frac{N^2}{c^2}(\rho\overline{w}) = 0$$

Note that the vertical velocity is now in height, not pressure coordinates. For constant Brunt-Vaisala frequency, N, each mode will be sinusoidal and its corresponding wave speed can be diagnosed from its eigenvalue. We project the usual WTG forcing onto these modes, but the damping time constant, τ_n, of each nth mode varies according to its wave speed, c_n. Since c_n is inversely proportional to n, the gravest spectral mode is damped most quickly, while modes associated with larger n are damped more slowly, yielding:

$$\rho\overline{w} = \sum_{n=1}^{\infty} \frac{A_n}{n} \sin\left(\frac{n\pi z}{H}\right)$$

$$A_n = \frac{2}{H} \int_0^H \frac{\rho\left(\overline{\theta_v} - \overline{\theta_v^{\text{ref}}}\right)}{\left(\frac{\partial\overline{\theta_v}}{\partial z}\right)\tau_1} \sin\left(\frac{n\pi z}{H}\right) dz$$

here, H is the specified height of the tropopause, A_n is the normalized projection of the WTG forcing onto the spectral modes, and τ_1 is the damping time constant of the first, or gravest, mode. Since modes of larger n will generally have smaller magnitude due to the linear scaling of τ_n with n, we numerically implement the Spectral WTG method by considering only the first 20 terms of the infinite series. This led to negligible truncation error (not shown). As with the WTG method, we place a lower limit of 2 K km^{-1} on the absolute value of the static stability, $\frac{\partial\overline{\theta_v}}{\partial z}$.

2.2. Model Configuration

The WTG, DGW, and Spectral WTG methods all require some choice of a reference temperature profile. Since circulation implies the horizontal advection of moisture (discussed in more detail below), we must also determine a reference moisture profile. To replicate the setup used in Daleu et al. (2016), we obtain the reference temperature and moisture profiles by running SCAM6 in RCE (i.e., imposing zero vertical velocity) for a uniform SST of 300 K, a value intended to be representative of the tropical average. Starting from a moist adiabatic temperature profile with uniform 70% Relative humidity (RH), we run SCAM6 in RCE for 300 days and average over the final 100 days. In any runs that explore different convection and radiation schemes, we also use these settings to generate distinct RCE reference temperature and moisture profiles to ensure consistency between the modeled column and the reference mean tropical state. In all cases, horizontal wind speed is set to a vertically uniform value of 5 m s^{-1}, a prescription which does not affect the dynamics of convection, but plays an important role in computing surface fluxes (Daleu et al., 2015, 2016). All RCE reference profiles assume a uniform SST of 300 K.

As in Daleu et al. (2016), this study assumes no horizontal advection of temperature. Thus, the temperature ($\overline{\theta_v}$) tendency due to LS advection can be written as:

$$\left(\frac{\partial\overline{\theta_v}}{\partial t}\right)_{LS} = -\overline{\omega}\frac{\partial\overline{\theta_v}}{\partial p}$$

Moisture ($\overline{q_v}$) is treated differently and instead is subject to a one-way "lateral entrainment" described by Raymond and Zeng (2005). In addition to vertical advection by $\overline{\omega}$, moisture is horizontally advected into the column by local flow convergence, yet is not altered at levels of local flow divergence. We thus write our LS advective moisture tendency as:

$$\left(\frac{\partial \overline{q_v}}{\partial t}\right)_{LS} = -\overline{\omega}\frac{\partial \overline{q_v}}{\partial p} + \max\left(\frac{\partial \overline{\omega}}{\partial p}, 0\right)\left(\overline{q_v^{\text{ref}}} - \overline{q_v}\right)$$

Daleu et al. (2016) and many other studies (Herman & Raymond, 2014; Raymond & Sessions, 2007; Sessions et al., 2010; S. Wang et al., 2013) use this "lateral entrainment" of moisture, whereas other studies used different representations of the horizontal advection of moisture (Sobel & Bellon, 2009; Sobel et al., 2007; S. Wang & Sobel, 2012).

Daleu et al. (2016) specifies an idealized radiative cooling profile to isolate interactions between convection and LS dynamics in each model. They prescribed a uniform 1.5 K day^{-1} cooling rate below 200 hPa, relaxed the temperature above 100 hPa to 200 K, and linearly interpolated between these cooling rates between 100 and 200 hPa according to the following formula:

$$\left(\frac{\partial T}{\partial t}\right)_{RC} = \begin{cases} -1.5 & \text{if } p \geq 200 \\ -1.5\left(\frac{p-100}{100}\right) - \alpha_T\left(\frac{200-p}{100}\right)(T-200) & \text{if } 100 < p < 200 \\ -\alpha_T(T-200) & \text{if } p \leq 100 \end{cases}$$

where p is in hPa, T is in K, and $\frac{\partial T}{\partial t}$ is in K per day. They set the constant α_T to 1 day^{-1}. For this study, we run cases using either the specified radiative cooling above or the interactive radiation package in SCAM6, a streamlined version of the rapid radiative transfer method (RRTMG) that derives from a correlated k-distribution (Lacis et al., 1979). We refer to cases run using specified radiation with the label "Rs" and refer to cases run using RRTMG, or fully interactive radiation, with the label "Ri."

SCAM6 uses a unified turbulence scheme, Cloud Layers Unified by Binormals, for shallow convection (Golaz et al., 2002) and the Zhang-McFarlane (ZM) scheme (Zhang & McFarlane, 1995) for deep convection. The ZM scheme allows an ensemble of convective-scale updrafts, and associated saturated downdrafts, to occur whenever the lower troposphere is conditionally unstable and the updrafts have sufficient buoyancy to penetrate the stable layer. These updrafts act to consume convective available potential energy (CAPE) in the convective layer at a specified time scale (2 hr).

One of the critical parameters in SCAM6's version of the ZM scheme is *zmconv_num_cin*, renamed δ_{CIN} for this study, which specifies the number of negative buoyancy levels that are allowed before the convective layer is capped and CAPE calculations are completed. This parameter determines the scheme's ability to overcome some amount of convective inhibition (CIN), which in turn often determines the level of convective cloud top. The default value of δ_{CIN} for SCAM6 is one, which sets the lowest neutral-buoyancy level of a pilot entraining plume to be the convective cloud top. This choice tends to cause the model to underestimate tropical variability and convective cloud top in global simulations (M. Wang & Zhang, 2018; Xie et al., 2018) and produces a shallow-convection prevailing regime in an idealized RCE framework (Hu et al., 2022). The default value of δ_{CIN} for SCAM6 is therefore being changed to three in future versions of CESM (personal communication). Thus, for this study we run cases using either $\delta_{\text{CIN}} = 1$, referred to as inhibited convection (Ci), or $\delta_{\text{CIN}} = 3$, referred to as uninhibited convection (Cu).

Finally, each of the parameterizations of LS dynamics contain parameters that specify the strength of the circulation response to a given temperature anomaly. In the WTG and Spectral WTG methods, τ and τ_1 set the time scale at which the column's temperature and the gravest spectral mode of the column's temperature, respectively, are relaxed back to the tropical mean. In the DGW method, ϵ plays a similar role, setting the mechanical damping coefficient with which the gravity waves are damped, notwithstanding that its units are the inverse of those of τ. The specified horizontal wave number, k, also plays a significant role in setting the strength of the circulation response, though this is left constant in the present study, set to 10^{-6} m^{-1} as in Daleu et al. (2016). Daleu et al. (2016) sets τ to 3 hr and ϵ to 1 day^{-1}. These are typical values used in previous studies (Daleu et al., 2012; Herman & Raymond, 2014; S. Wang & Sobel, 2011; S. Wang et al., 2013) and are chosen to produce comparable circulation responses to the same free tropospheric temperature anomaly in both the WTG and DGW method.

However, when using the circulation parameter values given in Daleu et al. (2016), the WTG and DGW methods in SCAM6 are led to erratic behavior, suggestive of numerical instability, perhaps due to the ZM convection scheme. For $\tau = 3$ hr, the WTG method yields vertical velocity and convective heating profiles that oscillate wildly, and, for $\epsilon = 1$ day^{-1}, the DGW method both crashes at an SST of 298 K and yields unrealistic S-shaped vertical velocity profiles at all other SSTs (see Results). This erratic behavior is robust across several different time step settings: 30 min, 20 min, and 10 min. 5 min time steps were also tested, though these result in undesired artifacts in the corresponding RCE simulations in Single Column Atmosphere Model (SCAM), consistent with findings from Hu et al. (2022). Thus, we instead achieve numerical stability by reducing the strength of the circulation's response to a given temperature anomaly. To do this, we increase τ and ϵ three- or five-fold from the Daleu et al. (2016) values. While the Spectral WTG method tends to be robust even at lower values of τ_1, we match τ_1 to τ in all cases considered. At these higher values of τ, ϵ, and τ_1, there is no significant change in results across the time steps we considered. Thus, all runs presented in this study use a somewhat arbitrary time step of 20 min. It is worth noting that, while increasing τ, ϵ, and τ_1 improves the numerical stability of the results, it also implies changes to some of the underlying physical reasoning inherent in these methods (see Discussion).

We run all cases using PLSD for 400 days under constant SST values of 298, 299, 300, 301, and 302 K. This range of SST values is comparable to the range used in Daleu et al. (2016). For each run, the steady-state is obtained by averaging the final 100 days. All runs presented in this study use 32 pressure levels, which has been used in the workhorse version of CESM2 (Danabasoglu et al., 2020). Several cases were also run using 60 pressure levels, though we observed no significant change in results under this increased vertical resolution. Some runs, especially for lower values of δ_{CIN}, τ, and ϵ, demonstrate multiple quasi steady-state equilibria. In all cases where we observe such behavior, we extend the run an additional 400 days to ensure no sizable variations occur in the steady-state quantities considered. We leave further exploration of such transient phenomena to future study. It is also worth mentioning that, in cases of interactive radiation (Ri), there is a seasonal cycle of insolation equivalent to that seen at the equator. However, when averaged over 365 days rather than 400 days, there is no significant change in any output parameters. Data and code are publically available (Cohen, 2023).

3. Results

3.1. Radiative-Convective Equilibrium

To begin, we consider the reference RCE state for each model configuration. We present quantities of interest from these RCE states in Table 1, which displays time-averaged precipitation and evaporation, and Figure 1, which displays time-averaged temperature, RH, and radiative and convective heating profiles.

As expected, the precipitation and evaporation in RCE are nearly identical (Table 1). The choice of specified versus interactive radiation scheme causes large differences in the time-averaged precipitation and evaporation. This result is not a surprise given that the idealized radiative cooling profile in Daleu et al. (2016) implies a substantially larger vertically integrated cooling than what the interactive scheme computes under these conditions, and this integrated cooling must be balanced by the sum of condensation heating and sensible surface heat flux in RCE. Differences in convection do not affect precipitation for the interactive radiation cases, and there is about a 6% change in precipitation between the Ci and Cu cases under specified radiation. Since we specify radiative cooling, and thus convective heating, to be 1.5 K day^{-1} below 200 hPa in the idealized radiation configuration, the changes appear to be primarily the result of relatively large upper tropospheric (above 200 hPa) temperature differences (Figure 1). The upper troposphere is substantially warmer when δ_{CIN} is set to 3, yielding greater radiative cooling and precipitation.

Figure 1 shows the time-averaged temperature, RH, radiative cooling, and convective heating in RCE for each of the convective and radiative conditions considered. One standard deviation in time (gray shaded areas) is shown for RiCu. Variances for other cases are similar in magnitude, save the specified radiative cooling profile in Rs. On the whole, the idealized radiation configuration yields a cooler troposphere than the interactive radiation case does, likely because the specified 1.5 K day^{-1} radiative cooling rate below 200 hPa is larger than what the interactive radiation scheme predicts for nearly all pressure levels (Figure 1). Relative humidity is computed with respect to liquid water, and it remains between 50% and 80% throughout the free troposphere for all RCE cases except the specified radiation with uninhibited convection case (RsCu), which shows less moisture in the mid troposphere.

Table 1
Precipitation and Evaporation (mm/Day) in Radiative Convective Equilibrium for Each Convective and Radiative Setting Considered

Precipitation/Evaporation	Inhibited convection (Ci)	Uninhibited convection (Cu)
Interactive Radiation (Ri)	2.74/2.72	2.74/2.74
Specified Radiation (Rs)	4.29/4.30	4.57/4.58

Note. Ri indicates use of the default interactive radiation scheme in SCAM6, Rs indicates use of specified radiative cooling, Ci indicates 1 level of CIN is tolerated in the convection scheme, and Cu indicates three levels of CIN are tolerated in the convection scheme.

3.2. Parameterized Large-Scale Dynamics Under Settings From GASS-WTG Intercomparison Project

We then simulate a column state in response to cooler and warmer SSTs than the reference 300 K RCE value (298, 299, 300, 301, and 302 K), holding the above RCE temperature and moisture profiles fixed as reference states for each of the parameterizations of LS dynamics. We first consider the RsCi case as a way to directly compare SCAM6 with Daleu et al. (2016). We also set the circulation parameters to the values given in Daleu et al. (2016), with τ_1 and τ set to 3 hr and ϵ set to 1 day^{-1}. Results are shown in Figure 2.

Under the WTG approximation, we expect a positive, monotonic relationship between SST and precipitation (Sobel & Bretherton, 2000). SSTs lower than that used to construct the RCE reference profiles should yield LS descent that suppresses convection, dries out the free troposphere, and allows relatively little precipitation. By contrast, higher-than-reference SSTs should yield LS ascent that enhances convection, moistens the free troposphere, and generates relatively heavy precipitation. In Figure 2, we check this expectation by plotting precipitation (blue) and evaporation (red) as a function of SST. While the Spectral WTG method performs as expected, the WTG and DGW methods not only do not follow this expectation (left column), but also demonstrate erratic behavior suggestive of numerical instability. This is shown in the simulated profiles of vertical velocity, temperature deviation from RCE, radiative cooling, convective heating, and RH for each method at each SST (Figure 2, right, colors scale from cool to warm). In the WTG method, both the vertical velocity and convective heating oscillate wildly, with the substantial variations in SST showing little effect on the solution. The runs using

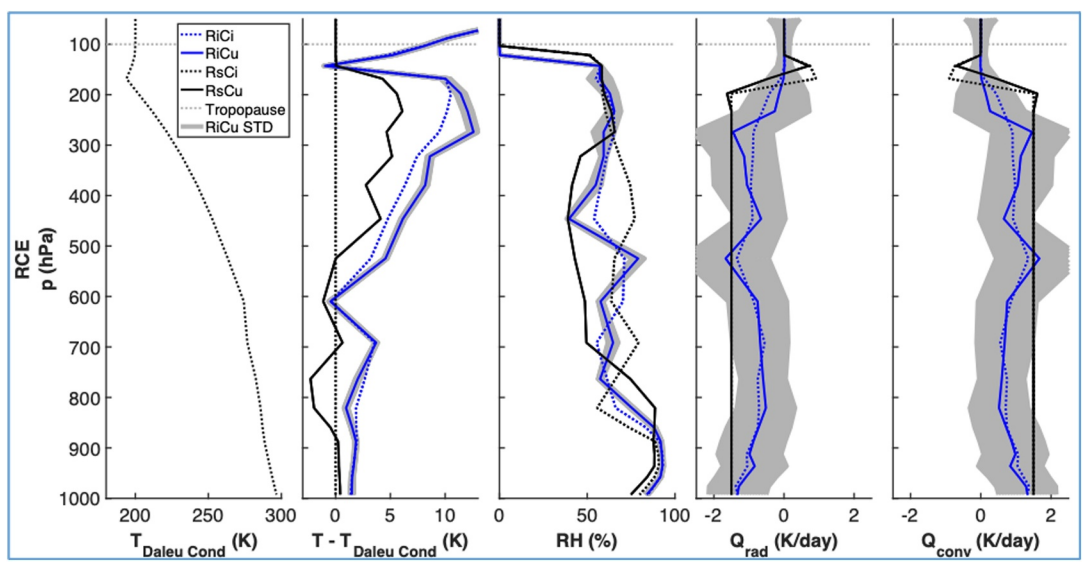

Figure 1. Column temperature, relative humidity, and convective and radiative heating in radiative convective equilibrium for each convective and radiative setting considered. Ri indicates use of the default interactive radiation scheme in single column atmospheric model, Rs indicates use of specified radiative cooling, Ci indicates 1 level of convective inhibition (CIN) is tolerated in the convection scheme, and Cu indicates three levels of CIN are tolerated in the convection scheme. The subscript "Daleu Cond" indicates use of all conditions given in Daleu et al. (2015, 2016), or RsCi. For reference, one standard deviation of model output over the last 100 days is shown for the RiCu case. The tropopause (100 hPa) is shown in dotted gray.

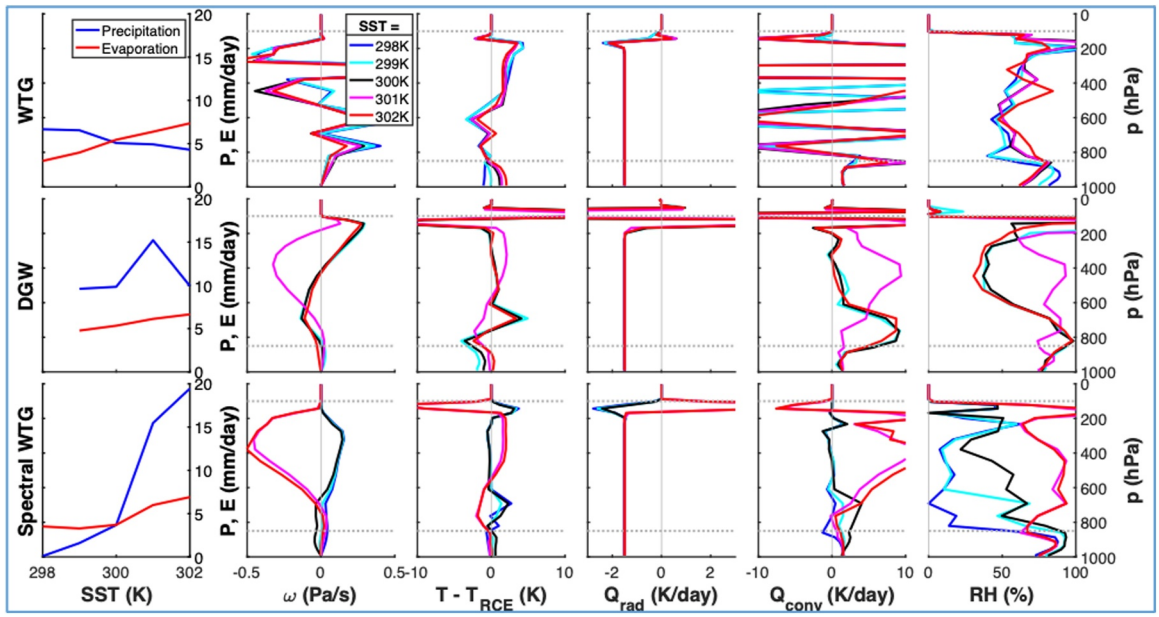

Figure 2. RsCi: Steady-state precipitation and evaporation rates and steady-state profiles of large-scale pressure velocity, temperature anomaly, relative humidity, and convective and radiative heating in weak temperature gradient (WTG), damped gravity wave, and Spectral WTG for τ_1 and τ set to 3 hr and ϵ set to 1 day^{-1} using specified radiative cooling and tolerating one level of convective inhibition in the convection scheme. The tropopause and boundary layer height are shown in dotted gray. Note that different scales are used for convective and radiative heating rates.

the DGW method behave a bit less erratically, but with numerical issues in the upper troposphere. This result is robust across all rigid lid DGW simulations, even when the height of the rigid lid is varied from 200 to 10 hPa. Additionally, the DGW method crashes at 298 K SST for this configuration, so no data is shown for this run. Finally, it is worth noting that the WTG and DGW methods demonstrate similarly erratic behavior for all other radiative and convective settings (RsCu, RiCi, and RiCu) when τ is set to 3 hr and ϵ is set to 1 day^{-1} (not shown). These numerical issues persist even when the vertical resolution is doubled or the time step is halved.

3.3. Parameterized Large-Scale Dynamics Under Relaxed Settings

If we increase the parameters used in Daleu et al. (2016) to weaken the strength of the circulation response, the WTG and DGW methods perform more stably and in line with our expectations based on Daleu et al. (2016). This is shown in Figure 3, which presents runs using three times the circulation parameters given in Daleu et al. (2016), with τ_1 and τ set to 9 hr and ϵ set to 3 days^{-1}. Radiative and convective settings are left unmodified (RsCi). Increasing τ, τ_1, and ϵ weakens the circulation response to a given temperature perturbation from the reference, which has the additional effect of smoothing the vertical velocity profiles. The WTG method (top) behaves more consistently with expectations; low SSTs yield gentle LS descent and light precipitation while high SSTs yield strong LS ascent and heavy precipitation. Qualitatively, the Spectral WTG method performs similarly to the WTG method for this configuration. However, it is able to sustain a larger magnitude of LS ascent for higher SSTs, making its steady-state precipitation for these runs substantially larger. The DGW method yields exceptionally dry conditions in this configuration; the expected deep convection and heavy precipitation for higher SST is not achieved. It is also worth noting that some grid-scale oscillation is observed for low SST runs in the upper tropospheric RH profiles of the DGW and Spectral WTG methods.

If we increase the circulation parameters given in Daleu et al. (2016) even further to five times their original values (with τ_1 and τ set to 15 hr and ϵ set to 5 days^{-1}), again leaving radiative and convective settings unmodified, the DGW method begins to yield heavy precipitation for higher SST (Figure 4). Thus, for this configuration, all methods behave qualitatively similarly, following the broad theoretical expectation that low SST will yield LS descent and low precipitation while high SST will yield LS ascent and heavy precipitation. However, the SST at which heavy precipitation begins to occur varies substantially from method to method, with this transition occurring at the expected 300 K SST for the Spectral WTG method, 301 K SST for the WTG

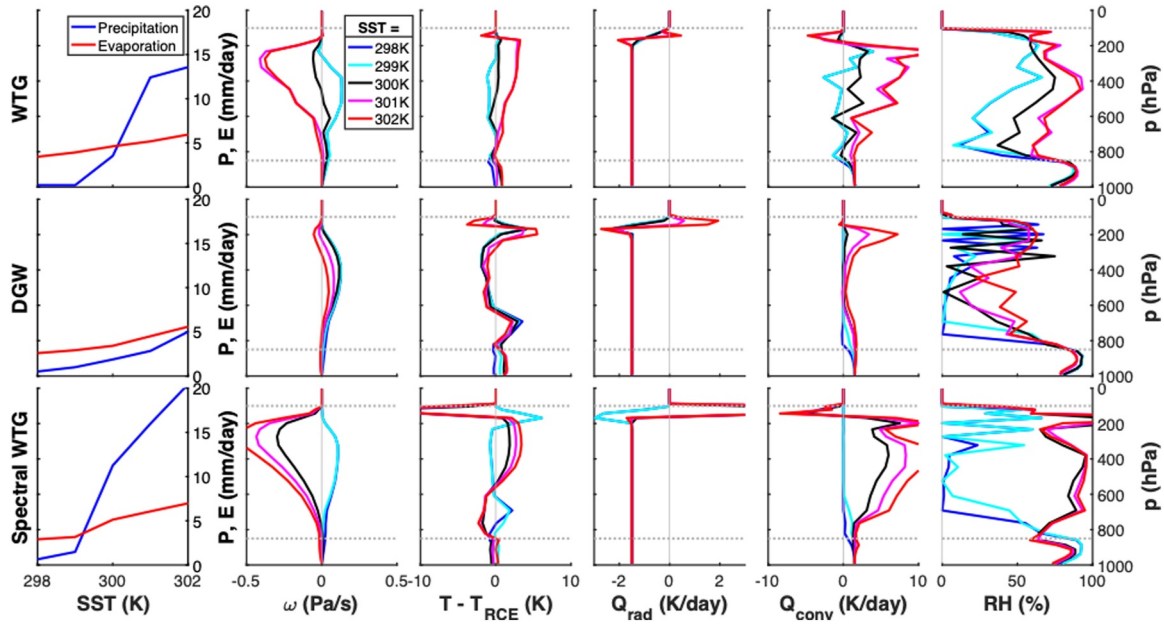

Figure 3. RsCi: Same as in Figure 2, but with τ_1 and τ set to 9 hr and ϵ set to 3 days^{-1}.

method, and 302 K SST for the DGW method. In addition, vertical velocity profiles tend to be more top-heavy for the WTG method and Spectral WTG method than for the DGW method, a difference also observed in Daleu et al. (2016) and Romps (2012). Vertical velocity profiles are smoother for the Spectral WTG and DGW methods than for the WTG method because the second order wave equation in the DGW method and the mode-dependent damping in the Spectral WTG method allow temperature perturbations in the column to produce non-local responses in ω in ways that favor larger vertical scales in the latter (Herman & Raymond, 2014; Kuang, 2008; S. Wang et al., 2016). However, while these smoothing effects are observed in the convective heating profiles and the temperature deviation from RCE, they do not appear to smooth the column's RH profile. This oscillatory structure of upper-tropospheric moisture is also observed in Hu et al. (2022), though that study focused on SCAM

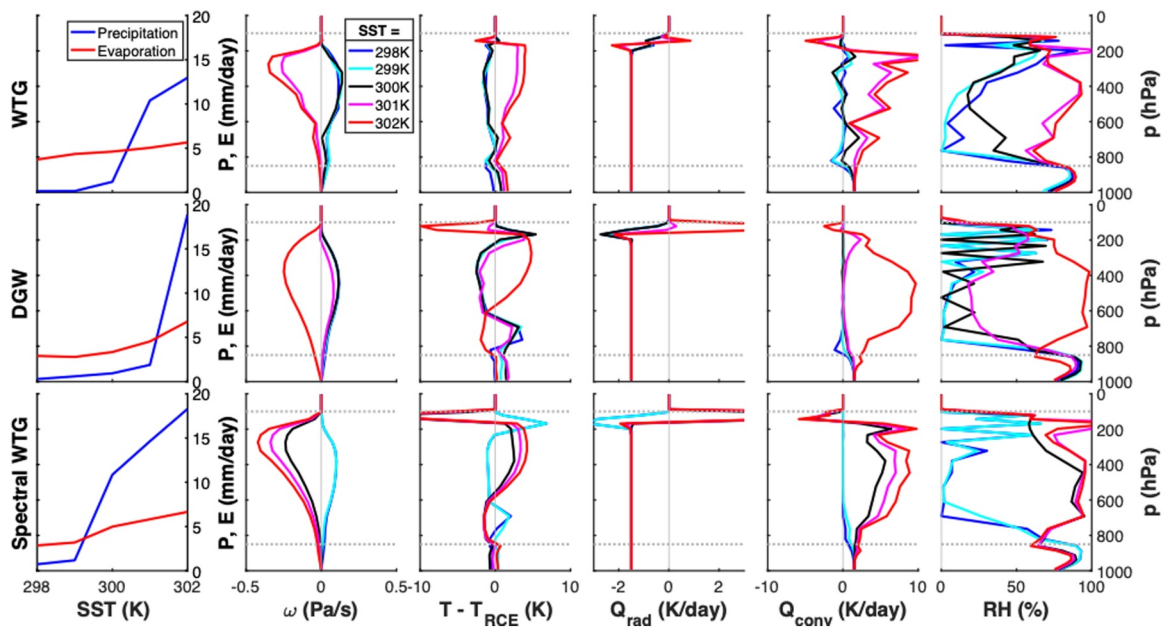

Figure 4. RsCi: Same as in Figures 2 and 3, but with τ_1 and τ set to 15 hr and ϵ set to 5 days^{-1}.

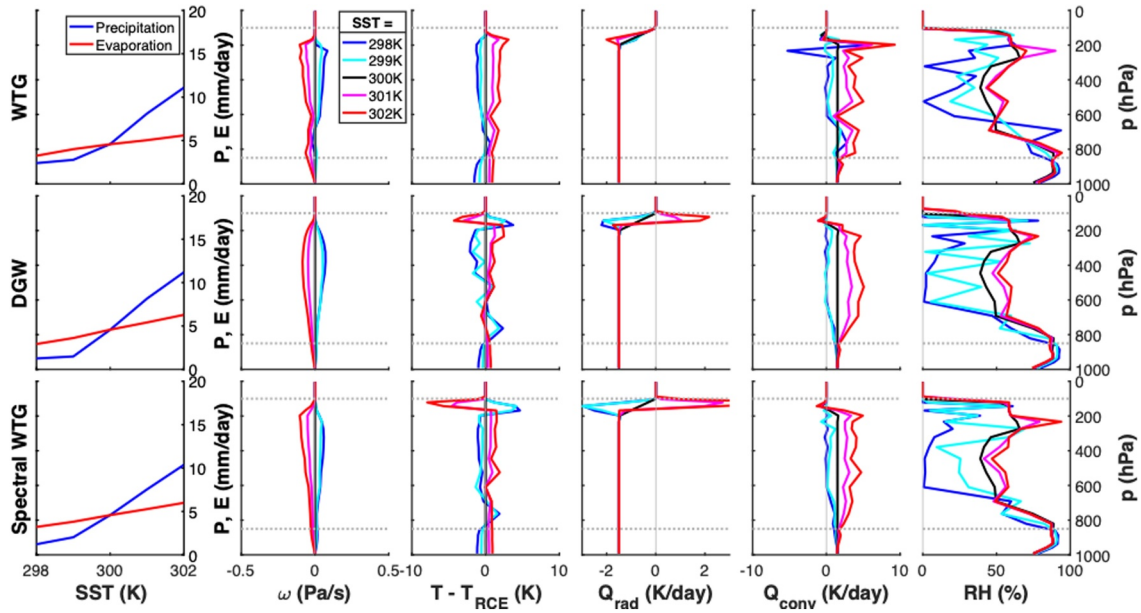

Figure 5. RsCu: Same as in Figure 4, but tolerating three levels of convective inhibition in the convection scheme.

under RCE, not under PLSD. Nonetheless, the hypothesis posed in Hu et al. (2022)—that these oscillations in upper tropospheric moisture are caused by variations in convective height—is likely still relevant under PLSD at low SST.

The temperature deviation from the RCE reference profile tends to follow a similar structure across all methods. Temperature deviations across the mid troposphere are of opposite sign as the LS pressure velocity (almost by design), with positive temperature anomalies being associated with LS ascent and negative temperature anomalies being associated with LS descent (Figure 4). However, in the upper and lower troposphere (above ∼200 hPa and below ∼600 hPa, respectively), we observe the opposite relationship for the DGW and Spectral WTG methods: LS ascent is associated with negative temperature anomalies and LS descent is associated with positive temperature anomalies. It is worth noting that this inverted relationship between the temperature anomaly and the LS pressure velocity in the upper and lower troposphere is much weaker (if perhaps non-existant) for the WTG method. In the WTG method, the LS pressure velocity is purely driven by the local temperature anomaly. By contrast, the wave equation in the DGW method and the spectral decomposition in the Spectral WTG method enable temperature anomalies to affect the LS pressure velocity non-locally.

Next, we consider configurations with different radiative and convective settings, all using circulation parameters with five times the values given in Daleu et al. (2016), a setting that most consistently produces results in line with expectations. To begin, we consider RsCu, where the number of tolerated negative buoyancy regions in the convective scheme (δ_{CIN}) is increased from one to three, but the radiation is still specified (Figure 5). In this case, all methods perform remarkably similarly to one another, transitioning from light to heavy precipitation at the same SST. Relative humidity and vertical velocity profiles also look remarkably similar across methods. However, in cases where deep convection does occur, convective ascent is generally weaker and the mid troposphere thus contains notably less moisture than it does for RsCi. We will show below that these differences in the magnitude of the vertical velocity likely stem more from differences in the RCE reference profiles than from differences in the behavior of the convective scheme for a fixed reference profile. Under less-inhibited convection settings (Cu), the RCE profile is more statically stable (Figure 1), meaning the free tropospheric temperature anomalies are smaller and the circulation is weaker (see Discussion for details).

Next, we consider configurations using SCAM6's default interactive radiation scheme (RRTMG) rather than the idealized radiative cooling profile from Daleu et al. (2016). We present results for RiCi (Figure 6) and RiCu (Figure 7). Runs with lower SSTs tend to yield greater radiative cooling in the majority of the troposphere, primarily due to lower cloud fraction and thus reduced shortwave heating (not shown). As with the idealized

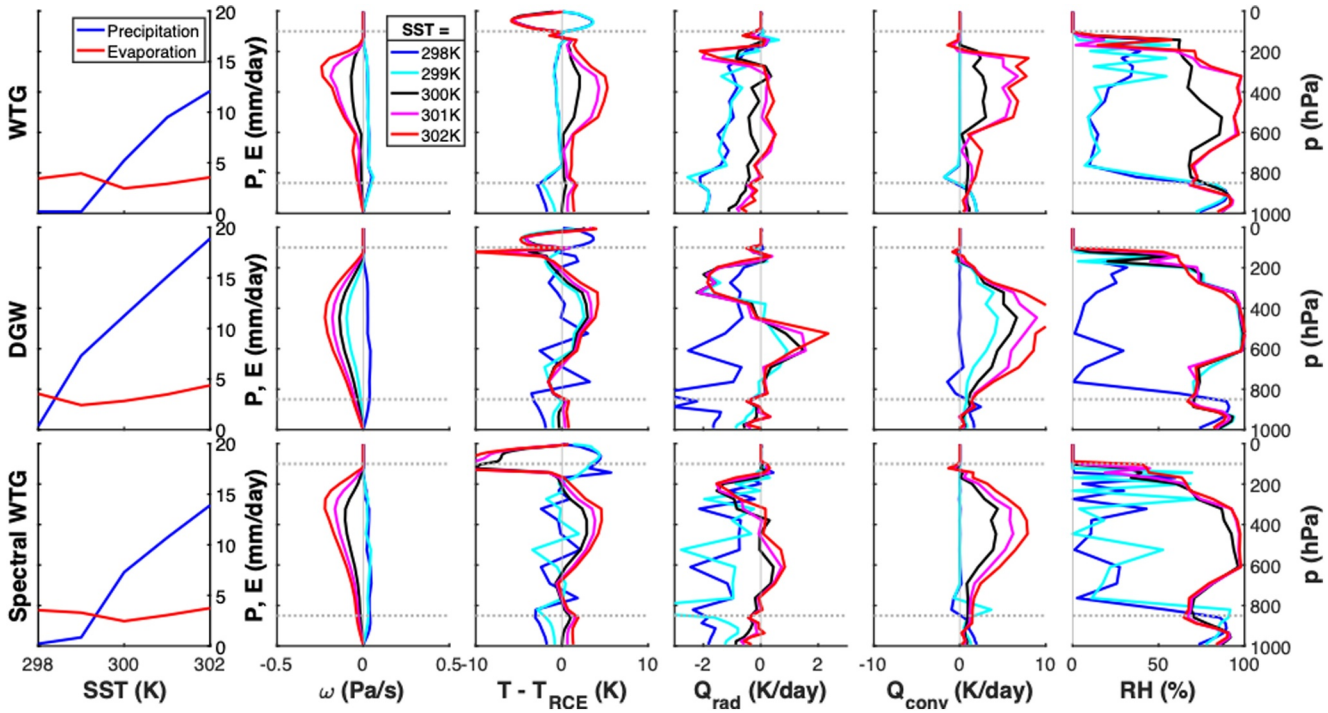

Figure 6. RiCi: Same as in Figure 4, but using interactive radiative cooling.

radiation cases, using $\delta_{\mathrm{CIN}} = 3$ tends to yield weaker convective ascent than using $\delta_{\mathrm{CIN}} = 1$. However, this difference is smaller when using interactive radiation than when using specified radiation.

Sharp vertical oscillations in convective heating suggest numerical issues in the 302 K SST run for the WTG method in Figure 7 (RiCu). In fact, while nearly all cases using circulation parameters with five times the values given in Daleu et al. (2016) performed reasonably, the WTG method performed somewhat strangely under interactive radiation and uninhibited convection. The expected monotonic relationship between SST and

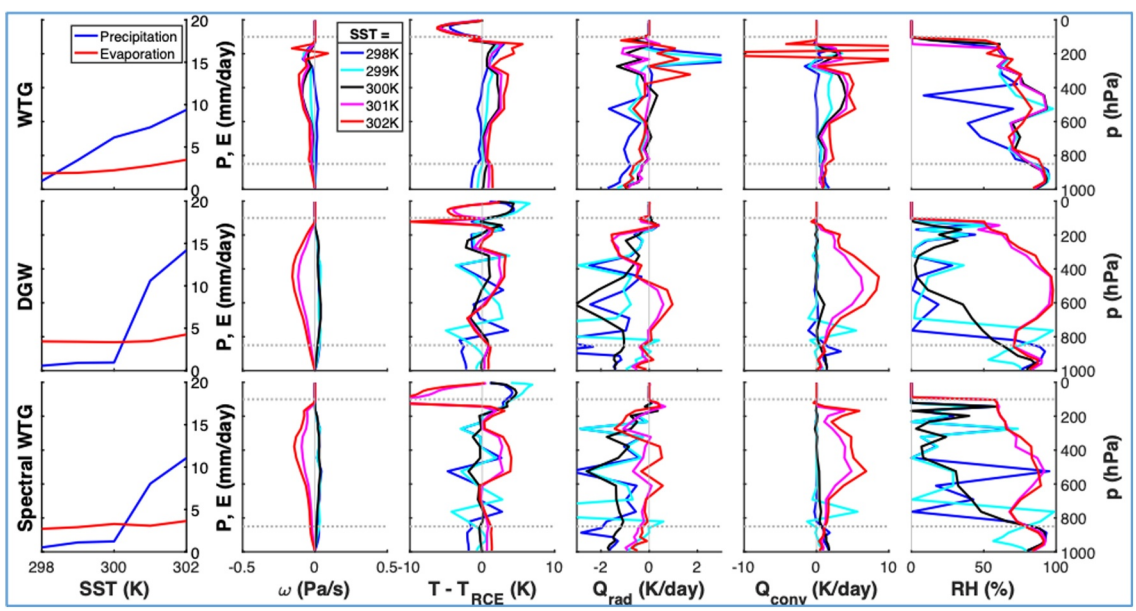

Figure 7. RiCu: Same as in Figure 5, but using interactive radiative cooling.

precipitation is apparent, but the method tends to favor deep convection. Even at the lowest SST, LS descent is weaker than in the other methods, and correspondingly the troposphere remains relatively moister.

Across configurations, there is significant variation in the "pickup" SST at which heavy precipitation begins to occur. Perhaps most notable in this regard is the DGW method; for RsCi (Figure 4) heavy precipitation begins to occur at an SST of 302 K, while for RiCi (Figure 6) this transition occurs at an SST of 299 K. The WTG approximation would suggest that, all else being equal, precipitation should exceed the RCE value for SSTs warmer than the reference value (interpreted as representing the tropical mean) and should be less than the RCE value for SSTs colder than the reference. Thus, we would expect a pickup SST of about 300 K for all cases considered in this study. The observed deviation from this expectation suggests that deep convection is being triggered (or suppressed) by mechanisms other than the parameterized LS circulation.

4. Discussion

4.1. Comparison to GASS-WTG Intercomparison Project

One of the main goals of this study is to compare the performance of SCAM6 under PLSD to those of the models in the GASS-WTG Intercomparison project (Daleu et al., 2016). Figure 8 compares precipitation versus SST curves for the WTG, DGW, and Spectral WTG methods in SCAM6 (under RsCi and RsCu) to the range of values seen in SCMs and CRMs in Figure 3 of Daleu et al. (2016). For circulation parameters equal to those used in the GASS-WTG Intercomparison project (left), the WTG and DGW methods are numerically unstable in SCAM6 and thus the relationship between SST and precipitation is not physically reasonable.

However, if key circulation parameters τ and ϵ are increased fivefold to 15 hr and 5 days^{-1} respectively (right), the circulation response to a given free tropospheric temperature anomaly decreases and the stability of the solutions is improved. These "relaxed" simulations produce the expected steep transition from light precipitation at low SST to heavy precipitation at high SST, yielding SST-precipitation curves which fall within the range of values seen in the SCMs considered in Daleu et al. (2016). In addition, the magnitudes and shapes of the vertical velocity profiles produced by the WTG and DGW methods in SCAM6 under relaxed settings likewise fall within the range of values seen in the SCMs considered in the GASS-WTG Intercomparison project (not shown).

However, it is worth noting that weakening the circulation response to temperature perturbations by increasing τ and ϵ does imply changes to the physical reasoning used to justify and interpret these methods. Since the elimination of temperature gradients in the tropics is a consequence of gravity waves, the time scale τ, for example, has been interpreted as the time it takes for the deepest dry gravity wave mode to traverse a given horizontal distance. By increasing τ and ϵ three- or five-fold, we are increasing the implied horizontal scale of the domain represented by the SCM a multiple of three or five as well. The resulting horizontal relaxation scales ($\sim$1,600 km for τ_1 and τ set to 9 hr and ϵ set to 3 days^{-1} and $\sim$2,600 km for τ_1 and τ set to 15 hr and ϵ set to 5 days^{-1}) are correspondingly greater than those implied by the smaller values used in Daleu et al. (2016).

The Spectral WTG method, in contrast to the WTG and DGW methods, achieves the expected relationship between SST and precipitation at all τ_1 considered. Consistent with Herman and Raymond (2014), we suggest that the relative robustness of the Spectral WTG method in SCAM6 stems from its wavenumber-dependent relaxation of the tropospheric temperature anomalies, which emphasizes the effect of smoother low wave number gravity wave modes and relaxes temperature anomalies not locally but via a column-average. Thus, the Spectral WTG method can integrate across grid-scale discontinuities, making them less likely to adversely affect the resulting circulation.

4.2. Role of Static Stability Under Radiative-Convective Equilibrium

The overall strength of the LS circulation for given radiative and convective settings remains sufficiently constant across all LS parameterizations to allow us to investigate the effect of modifying the radiation and convection schemes. Most notably in this regard, decreasing δ_{CIN} (Cu $\rightarrow$ Ci) tends to increase the strength of the circulation response, more so in the case of idealized radiation than for interactive radiation.

The increase in circulation strength when δ_{CIN} is decreased can be explained by variations in the static stability of the RCE temperature profile from one configuration to another (Figure 9). In RCE under inhibited convection settings (Ci, $\delta_{\mathrm{CIN}} = 1$), deep convection cannot grow as easily nor consume as much available instability (Hu

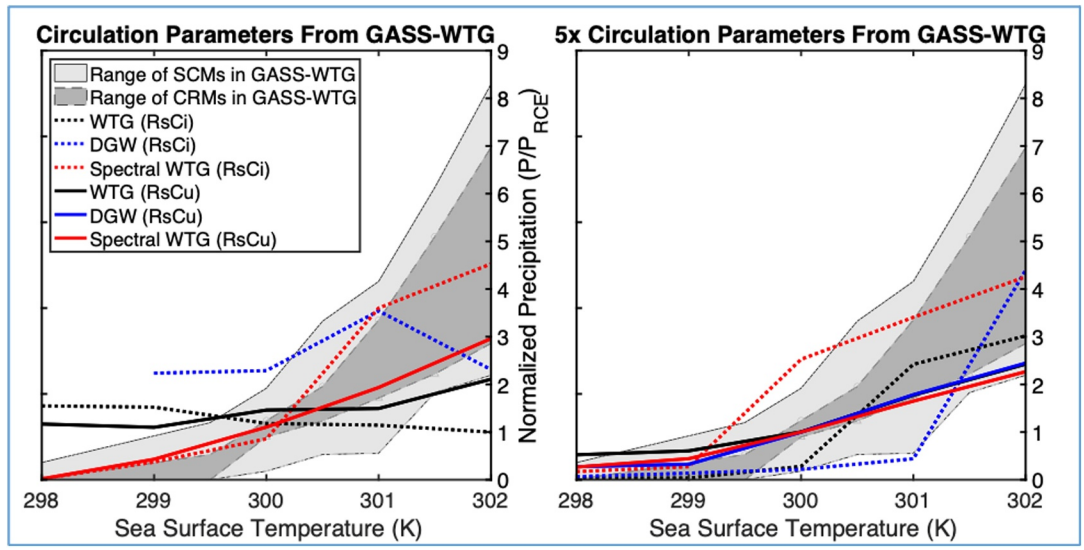

Figure 8. Normalized precipitation versus sea surface temperature curves for the weak temperature gradient (WTG), damped gravity wave (DGW), and Spectral WTG methods in SCAM6 under RsCi and RsCu. Curves are shown for τ_1 and τ set to 3 hr and ϵ set to 1 day^{-1} (left) and for τ_1 and τ set to 15 hr and ϵ set to 5 days^{-1} (right). They are compared to the range of values seen in single column models (light shading) and cloud resolving models (dark shading) in Daleu et al. (2016). For ϵ set to 1 day^{-1}, the DGW method crashes at 298 K for RsCi and at all SSTs for RsCu, so these results are not plotted.

et al., 2022). This results in a less statically stable tropospheric temperature profile than that under uninhibited convection settings (Cu, $\delta_{\mathrm{CIN}} = 3$). However, at high SST (302 K) under PLSD, convection can grow deeply regardless of the convective settings. In this case, the balance in the temperature equation is between the convective heating and the vertical advection by the LS circulation, since radiative cooling is much smaller than convective heating (Figures 4 and 5). The steady-state solution in the column is effectively a time-averaged balance between two forcings: the convection scheme acting to approximately relax the column's temperature profile to an entraining moist adiabat set by the locally warm SST and the circulation pushing the column's temperature towards the RCE reference profile. Thus, if the RCE profile is less statically stable (as it is under inhibited convection settings, Ci), there will be a larger temperature difference between this RCE profile and the entraining moist adiabat towards which the convection scheme is relaxing (Figure 9). This larger temperature difference introduces more CAPE into the column for a given circulation strength, yielding more LS ascent, more convection, and more steady-state precipitation.

In addition, lower static stability in the column means that a larger vertical velocity is needed to create the same temperature tendency. Thus, even at low SST where convection is nearly absent, decreasing δ_{CIN} (Cu $\rightarrow$ Ci) increases the strength of the (subsiding) circulation, though it is of opposite sign. In these cases, the energetic balance is primarily between the radiation and the circulation, so a lower column static stability under Ci requires a stronger downward LS vertical velocity (Figures 4 and 5) for similar deviation from the RCE temperature (Figure 9). We display this effect in Figure 9 for the WTG method; equivalent plots for the DGW and Spectral WTG methods are qualitatively similar (not shown). Under WTG, the time-averaged potential temperature profile at 302 K SST is much further from the RCE potential temperature profile for inhibited convection ($\delta_{\mathrm{CIN}} = 1$, red dotted profile) than for uninhibited convection ($\delta_{\mathrm{CIN}} = 3$, red solid profile). This increased competition between the circulation and the convection scheme yields a stronger circulation response and thus more steady-state precipitation.

How can we ensure the differences in circulation and precipitation described above are due to differences in the RCE reference states and not to the effect of δ_{CIN} on the convection directly? At high SST (302 K), the time-average top of convection (defined as the level at which the convective heating vanishes) is near the tropopause for all methods, regardless of the value of δ_{CIN} (not shown). However, in RCE, the top of convection is much lower for inhibited convection than for uninhibited convection. Since δ_{CIN} affects the convection scheme chiefly by setting the top of convection, this means that, at least in a time average sense, δ_{CIN} has a minimal effect

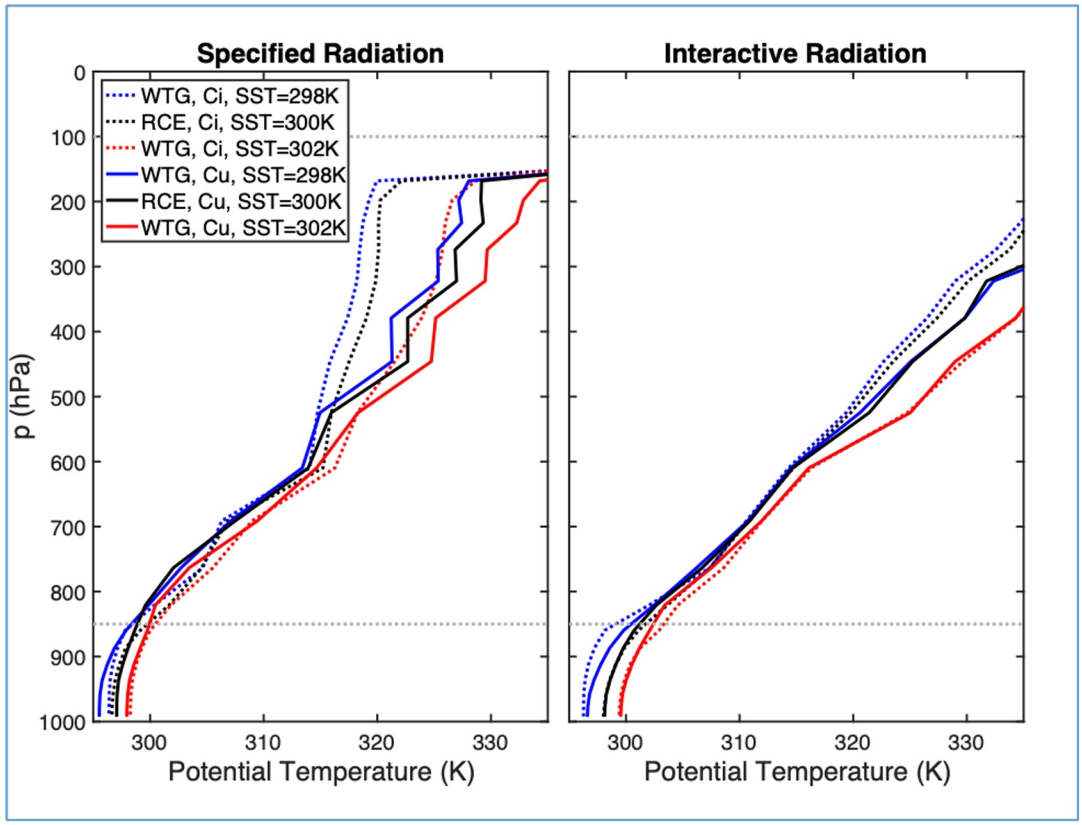

Figure 9. Time-averaged potential temperature profiles for radiative convective equilibrium at 300 K sea surface temperature (SST) (black), and weak temperature gradient at 298 K SST (blue) and 302 K SST (red) for τ set to 15 hr and tolerating either one (dashed) or three (solid) levels of convective inhibition in the convection scheme. Results are shown for specified radiation (left) and interactive radiation (right).

on the column itself at high SST, and mostly affects the column through its modification to the RCE reference profile. These results are in line with findings from Hu et al. (2022).

We suggest that the above argument holds for interactive radiation cases as well (Figure 9, right). As in the specified radiation cases, increasing δ_{CIN} tends to increase the static stability of the reference RCE profile (Figure 9, right) and decrease the precipitation and strength of the circulation response at high SST (Figure 10), even though this effect is less extreme.

Figure 10 shows the relationship between a bulk measure of RCE static stability (the temperature drop from 700 to 300 hPa) and the 302 K SST precipitation under both specified and interactive radiation. In both cases, precipitation at 302 K SST increases as the temperature drop from 700 to 300 hPa in the RCE reference state increases, that is, the static stability decreases. While the change in static stability in RCE across CIN parameters is smaller under interactive radiation than that under specified radiation, the effect on precipitation at high relative SST is qualitatively the same. Moreover, the top of convection is again relatively independent of δ_{CIN} at high SST (not shown) and convective heating likewise dominates over radiative cooling. Still, the fact that radiation is interactive leaves open the possibility that differences in radiative effects in the column itself play a role in setting the strength of the circulation response.

5. Conclusions

This study has implemented various parameterizations of LS dynamics into NCAR's single column atmospheric model SCAM6, with the purpose of both furthering development of NCAR's CESM and exploring the mechanisms that drive steady-state tropical precipitation. We implemented three parameterizations of LS dynamics into SCAM6: the WTG method (Raymond & Zeng, 2005), the DGW method (Kuang, 2011), and the spectral WTG

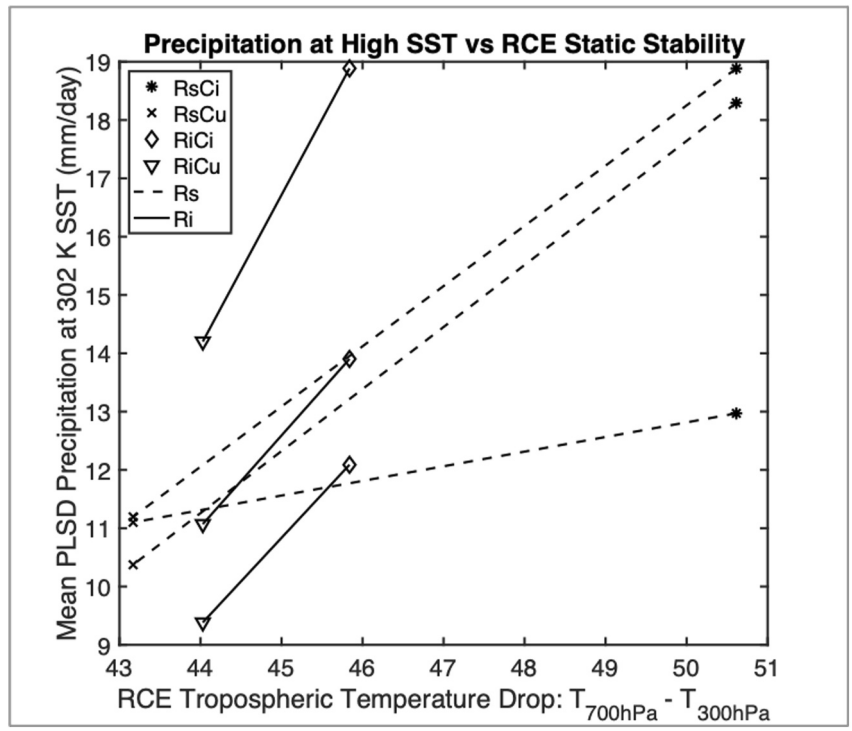

Figure 10. Mean precipitation at 302 K sea surface temperature (SST) for all parameterized large-scale dynamics (PLSD) methods versus the temperature change from 300 to 700 hPa in radiative convective equilibrium (RCE). Higher tropospheric temperature change in RCE (at 300 K) indicates greater lapse rate and lower static stability in the RCE reference profile, causing greater time-averaged precipitation under PLSD at high SST (302 K). Lines, dashed and solid, indicate changes from Cu to Ci across individual methods (weak temperature gradient (WTG), damped gravity wave, Spectral WTG).

(Spectral WTG) method (S. Wang et al., 2016). SCAM6 was run under a variety of convective and radiative settings with the same LS parametrization settings as in the GASS-WTG Intercomparison Project (Daleu et al., 2016) and with key LS circulation parameters relaxed.

The WTG and DGW methods lead to erratic behavior, with indications of numerical instability, in SCAM6 with the values of τ and ϵ used in the GASS-WTG Intercomparison project (Daleu et al., 2015, 2016). However, when these circulation parameters are increased fivefold, weakening the coupling between circulation and temperature, the WTG and DGW methods yield results qualitatively similar to those of Daleu et al. (2016), and reproduce the broad theoretical expectation that low SST will yield LS descent and low precipitation while high SST will yield LS ascent and heavy precipitation. The Spectral WTG method is more insensitive to changes in the circulation, radiation, and convection schemes, showing both greater numerical stability and a more consistent transition from light to heavy precipitation, always at or near the RCE SST, as expected.

For a given radiative and convective setting, all parameterizations of LS dynamics produce similar circulation strengths and precipitation levels to each other at very high and very low SST. In contrast, circulation strength and precipitation level change substantially across convective settings. Changing δ_{CIN} from one (inhibited convection) to three (uninhibited convection) weakens the circulation and reduces precipitation at high SST. We demonstrate that this change is driven primarily by an increase in the static stability of the RCE reference profile.

Future study is needed to ascertain the relevance of these results to CESM model development and to steady state tropical precipitation more broadly. Next steps might include running CESM with inhibited ($\delta_{\mathrm{CIN}} = 1$) and uninhibited convection ($\delta_{\mathrm{CIN}} = 3$) to see if the GCM replicates the changes to circulation strength and precipitation at high SST that we observe in SCAM6. Furthermore, if these changes are replicated, what effect do they have on climatological features in the tropics such as the intertropical convergence zone and the Walker circulation? Does the static stability of the tropical average change with radiative forcing and is this associated with a change in the relationship between SST and precipitation?

While it is difficult to extrapolate from the simulations presented in this study, we can reasonably speculate that decreasing the barrier to convection (using $\delta_{CIN} = 3$ rather than $\delta_{CIN} = 1$) in CESM's convection scheme will yield a more realistic representation of tropical convection. Tropical temperature profiles tend to be broadly moist adiabatic, but the SCAM6 simulations using inhibited convection show sizable upper tropospheric deviations from a moist adiabatic (Figure 9) due to the fact that the convection scheme predicts a chronically low convective cloud top. Using uninhibited convection seems to alleviate this problem and could potentially prevent CESM from overestimating tropical circulation strength. This appears to be in line with findings from previous studies (Hu et al., 2022; S. Wang & Zhang, 2018; Xie et al., 2018). However, these predictions are speculative and should be explored in future research.

Similarly, it is still an open question why SCAM6 requires more relaxed circulation parameters than the SCMs considered in Daleu et al. (2016) for the WTG and DGW methods in order to behave well. Given the centrality of the deep convection scheme in setting the column's circulation and precipitation, it may be that the ZM scheme (which is not used by any of the other SCMs in Daleu et al.) is more prone to generating grid-scale discontinuities that can yield runaway feedbacks when paired with the WTG and DGW methods. Consistent with Herman and Raymond (2014), we suggest that the Spectral WTG method is perhaps more resilient to grid-scale discontinuities due to its wavenumber-dependent relaxation of column-averaged tropospheric temperature anomalies. In any case, our results suggest that the Spectral WTG method's insensitivity to changes in radiation, convection, and circulation make it better suited to use in SCAM6 and model development for CESM.

Data Availability Statement

All raw data and plotting code is available at https://zenodo.org/record/7999372.

Acknowledgments
This research was supported by National Science Foundation (NSF) Grant AGS-1933523. Isla Simpson and Andrew Gettelman were supported by the NSF National Center for Atmospheric Research which is a major facility sponsored by the National Science Foundation under Cooperative Agreement 1852997. I-Kuan Hu is supported by the NSF through Grant AGS-1839471. Computing resources were provided by NCAR's Computational and Information Systems Laboratory; Cheyenne's DOI is https://arc.ucar.edu/knowledge_base/75694398. The authors also thank two anonomous reviewers for very helpful reviews.

References

Charney, J. G. (1963). A note on large-scale motions in the tropics. *Journal of the Atmospheric Sciences*, *20*(6), 607–609. https://doi.org/10.1175/1520-0469(1963)020<0607:anolsm>2.0.co;2

Cohen, S. (2023). Raw data and plotting code for "implementation and exploration of parameterizations of large-scale dynamics in NCAR's single column atmosphere model SCAM6" [Dataset]. *Zenodo*. https://zenodo.org/record/7999372

Daleu, C., Woolnough, S., & Plant, R. (2012). Cloud-resolving model simulations with one and two-way couplings via the weak-temperature gradient approximation. *Journal of the Atmospheric Sciences*, *69*(12), 3683–3699. https://doi.org/10.1175/jas-d-12-058.1

Daleu, C. L., Woolnough, S. J., Plant, R. S., Sessions, S., Herman, M. J., Sobel, A. H., et al. (2015). Intercomparsion of methods of coupling between convection and large-scale circulation. Part I: Comparison over uniform surface conditions. *Journal of Advances in Modeling Earth Systems*, *7*(4), 1576–1601. https://doi.org/10.1002/2015ms000468

Daleu, C. L., Woolnough, S. J., Plant, R. S., Sessions, S., Herman, M. J., Sobel, A. H., et al. (2016). Intercomparsion of methods of coupling between convection and large-scale circulation. Part II: Comparison over non-uniform surface conditions. *Journal of Advances in Modeling Earth Systems*, *8*(1), 387–405. https://doi.org/10.1002/2015ms000570

Danabasoglu, G., Lamarque, J. F., Bacmeister, J., Bailey, D. A., DuVivier, A. K., Edwards, J., et al. (2020). The community earth system model version 2 (CESM2). *Journal of Advances in Modeling Earth Systems*, *7*. https://doi.org/10.1029/2019ms001916

Gettelman, A., Truesdale, J. E., Bacmeister, J. T., Caldwell, P. M., Neale, R. B., Bogenschutz, P. A., & Simpson, I. R. (2019). The Single Column Atmosphere Model version 6 (SCAM6): Not a scam but a tool for model evaluation and development. *Journal of Advances in Modeling Earth Systems*, *11*(5), 1381–1401. https://doi.org/10.1029/2018ms001578

Golaz, J.-C., Larson, V. E., & Cotton, W. R. (2002). A PDF-based model for boundary layer clouds. Part I: Method and model description. *Journal of the Atmospheric Sciences*, *59*(24), 3540–3551. https://doi.org/10.1175/1520-0469(2002)059<3540:apbmfb>2.0.co;2

Held, I. (2005). The gap between simulation and understanding in climate modeling. *Bulletin of the American Meteorological Society*, *86*(11), 1609–1614. https://doi.org/10.1175/bams-86-11-1609

Held, I. M., Hemler, R. S., & Ramaswamy, V. (1993). Radiative-convective equilibrium with explicit two-dimensional moist convection. *Journal of the Atmospheric Sciences*, *50*(23), 3909–3927. https://doi.org/10.1175/1520-0469(1993)050<3909:rcewet>2.0.co;2

Herman, M., & Raymond, D. (2014). WTG cloud modeling with spectral decomposition of heating. *Journal of Advances in Modeling Earth Systems*, *6*(4), 1121–1140. https://doi.org/10.1002/2014ms000359

Hu, I.-K., Mapes, B. E., Tulich, S. N., Neale, R. B., Gettelman, A., & Reed, K. A. (2022). Idealized simulations of the tropical climate and variability in the single column atmosphere model (SCAM): Radiative-convective equilibrium. *Journal of Advances in Modeling Earth Systems*, *14*(2), e2021MS002826. https://doi.org/10.1029/2021ms002826

Jakob, C., Singh, M. S., & Jungandreas, L. (2019). Radiative convective equilibrium and organized convection: An observational perspective. *Journal of Geophysical Research: Atmospheres*, *124*(10), 5418–5430. https://doi.org/10.1029/2018jd030092

Kuang, Z. (2008). Modeling the interaction between cumulus convection and linear gravity waves using a limited-domain cloud system-resolving model. *Journal of the Atmospheric Sciences*, *65*(2), 576–591. https://doi.org/10.1175/2007jas2399.1

Kuang, Z. (2011). The wavelength dependence of the gross moist stability and the scale selection in the instability of column-integrated moist static energy. *Journal of the Atmospheric Sciences*, *68*(1), 61–74. https://doi.org/10.1175/2010jas3591.1

Lacis, A., Wang, W. C., & Hansen, J. (1979). *Correlated k-distribution method for radiative transfer in climate models: Applications to effect of cirrus clouds on climate* (Vol. 2076, pp. 309–314). NASA Conference Publication.

Raymond, D., & Sessions, S. (2007). Evolution of convection during tropical cyclogenesis. *Geophysical Research Letters*, *34*(6), L06811. https://doi.org/10.1029/2006gl028607

Raymond, D. J., & Zeng, X. (2005). Modeling tropical atmospheric convection in the context of the weak temperature gradient approximation. *Quarterly Journal of the Royal Meteorological Society*, *131*(608), 1301–1320. https://doi.org/10.1256/qj.03.97

Romps, D. (2012). Numerical tests of the weak pressure gradient approximation. *Journal of the Atmospheric Sciences*, *69*(9), 2846–2856. https://doi.org/10.1175/jas-d-11-0337.1

Sessions, S., Sugaya, S., Raymond, D., & Sobel, A. (2010). Multiple equilibria in a cloud-resolving model using the weak temperature gradient approximation. *Journal of Geophysical Research*, *115*(D12), D12110. https://doi.org/10.1029/2009jd013376

Sobel, A., & Bellon, G. (2009). The effect of imposed drying on parameterized deep convection. *Journal of the Atmospheric Sciences*, *66*(7), 2085–2096. https://doi.org/10.1175/2008jas2926.1

Sobel, A., Bellon, G., & Bacmeister, J. (2007). Multiple equilibria in a single-column model of the tropical atmosphere. *Geophysical Research Letters*, *34*(22), L22804. https://doi.org/10.1029/2007gl031320

Sobel, A. H., & Bretherton, C. S. (2000). Modeling tropical precipitation in a single column. *Journal of Climate*, *13*(24), 4378–4392. https://doi.org/10.1175/1520-0442(2000)013<4378:mtpias>2.0.co;2

Sobel, A. H., Held, I. M., & Bretherton, C. S. (2002). The ENSO signal in tropical tropospheric temperature. *Journal of Climate*, *15*(18), 2702–2706. https://doi.org/10.1175/1520-0442(2002)015<2702:tesitt>2.0.co;2

Tompkins, A., & Craig, G. (1998). Radiative-convective equilibrium in a three-dimensional cloud-ensemble model. *Quarterly Journal of the Royal Meteorological Society*, *124*(550), 2073–2097. https://doi.org/10.1256/smsqj.55012

Wang, M., & Zhang, G. J. (2018). Improving the simulation of tropical convective cloud-top heights in CAM5 with CloudSat observations. *Journal of Climate*, *31*(13), 5189–5204. https://doi.org/10.1175/jcli-d-18-0027.1

Wang, S., & Sobel, A. (2011). Response of convection to relative sea-surface temperature: Cloud-resolving simulations in two and three dimensions. *Journal of Geophysical Research*, *116*(D11), D11119. https://doi.org/10.1029/2010jd015347

Wang, S., & Sobel, A. (2012). Impact of imposed drying on deep convection in a cloud-resolving model. *Journal of Geophysical Research*, *117*(D2), D02112. https://doi.org/10.1029/2011jd016847

Wang, S., Sobel, A. H., & Kuang, Z. (2013). Cloud-resolving simulation of TOGA-COARE using parameterized large-scale dynamics. *Journal of Geophysical Research*, *118*(12), 6290–6301. https://doi.org/10.1002/jgrd.50510

Wang, S., Sobel, A. H., & Nie, J. (2016). Modeling the MJO in a cloud resolving model with parameterized large-scale dynamics: Vertical structure, radiation, and horizontal advection of dry air. *Journal of Advances in Modeling Earth Systems*, *8*(1), 121–139. https://doi.org/10.1002/2015ms000529

Xie, S., Lin, W., Rasch, P. J., Ma, P., Neale, R., Larson, V. E., et al. (2018). Understanding cloud and convective characteristics in version 1 of the E3SM atmosphere model. *Journal of Advances in Modeling Earth Systems*, *10*(10), 2618–2644. https://doi.org/10.1029/2018ms001350

Zhang, G. J., & McFarlane, N. A. (1995). Sensitivity of climate simulations to the parameterization of cumulus convection in the Canadian Climate Centre general circulation model. *Atmosphere-Ocean*, *33*(3), 407–446. https://doi.org/10.1080/07055900.1995.9649539